Characterization, comparison, and choice of a commercial double-clad fiber for nonlinear endomicroscopy

Claire Lefort
Hussein Hamzeh
Frederic Louradour
Frédéric Pain
Darine Abi Haidar

Characterization, comparison, and choice of a commercial double-clad fiber for nonlinear endomicroscopy

Claire Lefort,[a,b] Hussein Hamzeh,[a] Frederic Louradour,[b,d] Frédéric Pain,[a] and Darine Abi Haidar[a,c,*]
[a]Paris-Sud University, Orsay, IMNC Lab, UMR 8165, France
[b]Limoges University, Limoges F-87060, France
[c]Paris 7-DENIS DIDEROT University, Paris F-75012, France
[d]XLIM Lab, UMR 7252, Limoges F-87060, France

Abstract. Several endomicroscope prototypes for nonlinear optical imaging were developed in the last decade for *in situ* analysis of tissue with cellular resolution by using short infrared light pulses. Fourier-transform-limited pulses at the tissue site are necessary for optimal excitation of faint endogenous signals. However, obtaining these transform-limited short pulses remains a challenge, and previously proposed devices did not achieve an optimal pulse delivery. We present a study of fibered endomicroscope architecture with an efficient femtosecond pulse delivery and a high excitation level at the output of commercially available double-clad fibers (DCFs). The endomicroscope incorporates a module based on a grism line to compensate for linear and nonlinear effects inside the system. Simulations and experimental results are presented and compared to the literature. Experimentally, we obtained short pulses down to 24 fs at the fiber output, what represents to the best of our knowledge the shortest pulse duration ever obtained at the output of a nonlinear endoscopic system without postcompression. The choice of the optimal DCF among four possible commercial components is discussed and evaluated in regard to multiphoton excitation and fluorescence emission. © *The Authors. Published by SPIE under a Creative Commons Attribution 3.0 Unported License. Distribution or reproduction of this work in whole or in part requires full attribution of the original publication, including its DOI.* [DOI: 10.1117/1.JBO.19.7.076005]

1 Introduction

In recent years, exploratory endomicroscopic examinations have become prevalent.[1] Indeed, bronchoscopy, colonoscopy, laryngoscopy, etc., are used to detect diseases as early as possible. The technique used is mainly miniaturized confocal microscopy terminated by an optical fiber for *in vivo* imaging deep inside organs. But it is still highly limited by the low level of beam penetration, high level of photodamage, and the only accessible mean of contrast, linear fluorescence. Consequently, surgeons appeal to physicists to convert this limited linear endomicroscope to a nonlinear one to obtain a higher penetration depth, reduced photo damage, and several complementary means of endogenous contrasts. The real time and direct study of cellular structure constituents, operation, and dysfunction without resorting to a surgical act is actually a clinical need. Thus, nonlinear high-resolution fiber imaging of *in vivo* organs or living animals at cellular or subcellular resolution has become progressively widespread over the last 20 years.[2,3] Multiphoton endomicroscopy allows nonlinear imaging contrast through endogenous second-harmonic generation (SHG) and two-photon fluorescence (TPF). Due to its flexibility and deep penetration depth, multiphoton endomicroscopy has the potential to replace invasive tissue excision or surgical biopsy by soft *in vivo* optical biopsy. Today, no endomicroscopic system is available to be commercialized because of several challenges.

The design of a multiphoton endomicroscope faces several major challenges:[4] (1) delivering near-infrared, high quality, single-mode, intense, and efficient femtosecond pulses at the endoscopic fiber output; (2) coupling the fiber output to a focusing miniaturized objective to achieve efficient excitation, high resolution, and a large field of view; (3) associating it with a scanning system; and (4) combining these excitation tools with an efficient collection system of the emitted multiphoton signals.

Among all unsolved difficulties mentioned above for the development of an endomicroscopic system, point (1), considering the choice of the endoscopic fiber, has not been studied or thoroughly explained. We have chosen to study the choice of the endoscopic fiber exclusively among commercially available ones.

Linear and nonlinear interactions between the fiber material and near-infrared femtosecond pulses are distorting and broadening them. Hence, these distorted pulses become inefficient for multiphoton excitation. Controlling these interactions is fundamental for efficient nonlinear excitation and, consequently, for better image quality. The increase of TPF and SHG signal levels as a result of short femtosecond pulse delivery[5,6] leads to reduced photo bleaching,[6] larger penetration depth,[6–8] and higher signal-to-noise ratio.[7] Linear effects are composed by additive orders of dispersion. Second-order dispersion (SOD) is usually compensated by passive dispersive line as a

*Address all correspondence to: Darine Abi Haidar, E-mail: abihaidar@imnc .in2p3.fr

grating lines,[9] hybrid systems,[10] or prism line.[11] These compensation methods often result in an output pulse duration that is not so far from the duration of laser pulses in the range of 100 fs. Significant higher orders, such as the third-order dispersion (TOD), are not compensated for, hence resulting in pulses that are still temporally broadened and far from being transform limited. Few passive dispersive systems are compensating simultaneously for SOD and TOD, such as chirp mirrors[11] or grism lines.[12–14]

Nonlinear interactions between femtosecond pulses and fiber material spectrally distort and broaden pulses. A solution is to use a specific architecture compensating simultaneously for linear and nonlinear effects.[9,13,15] Its importance for multiphoton imaging has been previously highlighted.[13] But this effect is often not compensated for[16] or eliminated, thus reducing the average power of excitation beam,[17] resulting in a low level of SHG or TPF signals.

The choice of the fiber for endomicroscopic multiphoton imaging system is also of a great importance for the final design. Among various fiber types, double-clad fibers (DCFs) have demonstrated many advantages.[16–26] They can achieve simultaneously efficient excitation through their core and efficient nonlinear signal collection through their inner cladding, hence allowing the use of a single fiber. Yet, the choice of the DCF among commercially available products has not been justified by an experimental or numerical analysis. Although, more confidentially, bundles of thousands of fiber cores have been experimentally studied.[8,27] But their use is complicated, mainly for the indispensable inhomogeneity of the cores, which perplex the excitation and their fragility. The utilization of hollow-core photonic band-gap fibers (HCPBGFs) has also been investigated for nonlinear endomicroscopic systems.[28] They are interesting in two ways: reducing nonlinearities and running around zero-dispersion wavelength, thus, requiring a low level of compensation. To allow simultaneous excitation beam output through the core and efficient nonlinear signal collection, these fibers must be associated with another fiber, specifically dedicated to multiphoton collection, or a double-clad HCPBGFs[29] could be used, but for the moment they are in development and are not commercially available.

This publication is dedicated to the comparison and the choice of the commercially available DCFs. It presents a comparison of four different commercial DCFs placed in our specific, homemade architecture for multiphoton excitation.[13,15] Their performances are evaluated and compared numerically and experimentally. Comparison is based on several characteristics of the pulses at the output of the endoscopic system: pulse duration, average output power, single-mode delivery, and production of nonlinear signal. The initial choice of the four commercially available DCFs was based on their performance found in the literature within endoscopic systems, all working at a central wavelength around 800 nm.[16–26] The importance of linear and nonlinear compensations is highlighted in each step.

2 Material and Methods

2.1 Experimental Femtosecond Fiber Delivery with Linear and Nonlinear Compensations Tested on the Production of Two-Photon Fluorescence Signals

The production of nonlinear signal at the DCF output is influenced by the pulse shape and duration. Short pulses lead to

higher nonlinear signal level, better penetration depth, reduced photo damage, and photo toxicity of biological tissues. That is why linear and nonlinear effects distort and enlarge pulses throughout the whole endoscopic system. These effects have to be compensated for to deliver the shortest possible femtosecond pulses at the DCF output. Since postcompression at the end of the fiber is impossible in an endoscope, the compensation is done before the fiber. For this purpose, Clark et al. compensation principle[15] is used.

The fiber system is composed of three elements. Figure 1(a) presents a schematic diagram of this setup. First, a tunable femtosecond Ti:Sapphire laser source (700–900 nm, 80-MHz repetition rate, 100-fs duration at full width at half maximum [FWHM]; Tsunami, spectra physics) is associated to a Faraday's isolator (ISO-05-800-BB, Newport) to avoid back reflections from the fiber to the laser cavity. Second, a compression and precompensation unit, placed before the DCF, allows to compensate dispersion and nonlinear effects in the endoscopic fiber. The compression and precompensation unit is composed of (1) a polarization maintaining single-mode fiber (SMF) of 0.5-m length, which is coupled to the laser and followed by (2) a grism-based anomalous stretcher named "grism line." A grism is a prism joined to a diffraction grating.[12–14] First, the SMF is spectrally and temporally broadening pulse by cumulated effects of self-phase modulation (SPM) and dispersion. Then, the dispersion compensation is governed by two degrees of freedom (DOF) of the grism line: the distance d between the two grisms and the incidence angle θ of the beam on the first grism.[13,14] Tuning these two parameters allows almost independent SOD and TOD compensation. In our experiments, these two parameters were adjusted for each DCF. Finally, pulses are launched into the endoscopic DCF where combined effects of nonlinearities and normal dispersions are temporally and spectrally compressing them.

In a first step, the grism line parameters were adjusted for each DCF; spectral and temporal characterizations were obtained at each DCF output, using a minispectrometer (Oriel Series IS 1, Newport, France) and an autocorrelator (Mini-PMT-NIR, AA11.08.01.03, APE). Figure 1(b) presents the spectra at the oscillator output and before the DCF input. Figure 1(c) presents the autocorrelation trace of the shortest pulse (24 fs), obtained at the endoscopic output.

In a second step, two-photon fluorescence excitation and collection through one of the four DCFs were measured using a fluorescent solution of Rhdoamine B sample (RhB, 10^{-5} M, Sigma Aldrich Fluka, Saint-Quentin Fallavier, France). The fluorescence is collected by the DCF inner cladding and delivered at the proximal position [Fig. 1(a)] where a dichroic mirror discriminates the fluorescence signal and the excited beam.

2.2 Selection of the Commercial Double-Clad Fiber

Regarding to the commercial DCFs used in the literature for building a nonlinear endomicroscopic system, four DCFs are mainly employed. Their parameters and corresponding literature references are summarized in Table 1. A first way to discriminate between them should be to consider several DCF parameters in order to optimize endomicroscopic system performances. Three of the four selected DCFs are classical step-index fibers with a doped core (potentially creating background signal) and an undoped inner cladding made from pure silica to create the necessary refractive index gap. These doping elements can potentially produce a noise from the fiber itself. The best
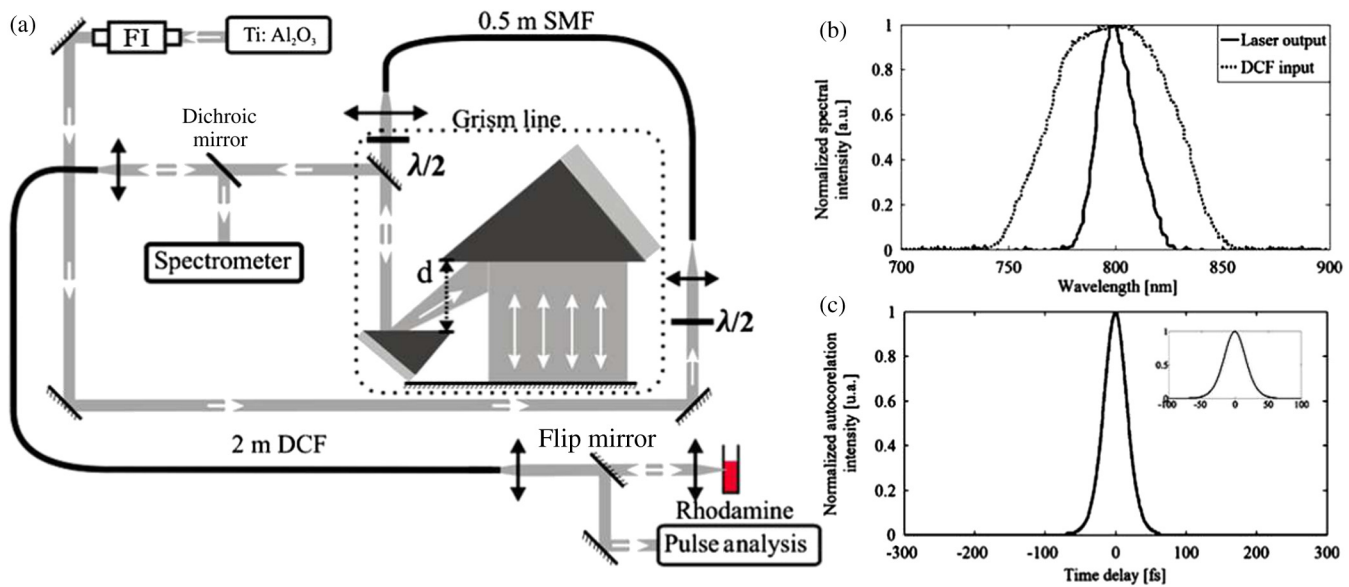
Fig. 1 (a) Testing bench for endoscopic DCFs. Ti: AL$_2$O$_3$: titan sapphire laser source. FI: Faraday isolator. $\lambda/2$: half-wave plate. Module of linear and nonlinear effects compensation with a single-mode fiber and a grism line. Spectral and temporal pulse analysis at DCFs output. TPF tested with rhodamine fluorophore at a DCF output. Fluorescence spectrally analyzed at the DCF input. Florescence discriminated from excitation beam with a dichroic mirror, (b) spectral characterization of beam at the laser output and before the DCF, (c) temporal pulse analysis at the laser output.

solution would be to utilize only pure silica in the fiber composition as in microstructured fibers. The last factor that affects performances is the fiber dimension. Considering the same distal focalization lens, the smaller the core size, the smaller the focal volume and, hence, the better the resolution.

Despite all the technical problems for fiber fabrication, the ideal DCF should have a relatively small core to achieve an indispensable single-mode excitation and to achieve high-spatial resolution using a miniaturized endoscopic lens. Regarding the numerical aperture (NA), the core must have a small NA in order to minimize aberrations in distal optics. The inner cladding must have a high NA in order to maximize collection efficiency of multiphoton signal from the sample. As we can observe in Table 1, a compromise is necessary in the choice of the DCF because none of these four fibers combine all the ideal parameters for efficient multiphoton excitation.

2.3 Numerical Simulations of Pulse Characteristics at Double-Clad Fiber Output

Another important point that should be considered is the production of nonlinear signal at the DCF output that is closely related to the pulse shape and duration. Numerical simulations were carried out to foresee the time characteristics of the light pulses

at the output of each DCF (Fibercore, Liekki, Crystal Fiber, Nufern) in our homebuilt architecture [Fig. 1(a)]. A custom-made MATLAB® program simulating pulse propagation in this architecture was used. It simulates the scheme composed of a laser source, a precompensation step, and a DCF. The simulation parameters are: (1) the initial pulse central wavelength and its corresponding pulse duration, (2) spectral bandwidth, (3) average power, (4) DCF fiber length, (5) its core diameter, and (6) grism line parameters (d and θ). The program simulates the pulse propagation in the fiber with all the significant orders of dispersion considering the spectral bandwidth after the first fiber [SOD, TOD, and fourth-order dispersion (FOD)], as well as nonlinear effects. For the simulation of the dispersive grism line, the user can set its structural properties (prism apex angle and glass composition, grating groove density) and the DOF (distance d between grisms and incident angle θ of the beam on the first grism). In our simulations, the central wavelength is fixed at 800 nm. The initial spectral bandwidth of oscillator is 10 nm at FWHM with 100-fs pulse duration. The lengths of the first and second fibers are respectively 0.5 and 2 m. The core diameter of the first fiber is 5 μm (simulating the 780HP fiber, Thorlabs), the groove density is 600 grooves/mm and the prism angle is 40 deg. The core diameter of the second fiber is set according to the studied DCF.

Table 1 Characteristics of the four considered double-clad fibers (DCFs).

Manufacturer	Reference	Core (μm)	Core NA	Inner cladding (μm)	Inner cladding NA	Structure
Fibercore	SMM900	3.6	0.19	100	0.25	Step index
Liekki	Passive-6/125DC-PM	5.5	0.15	125	0.46	Step index
Crystal Fiber	DC-165-16 P	16	0.04	163	0.64	Microstructured
Nufern	SM-9/105/125-20A	9	0.12	105	0.2	Step index

The simulation program provides the pulse characteristics at the exit of the DCF, including their temporal shape and duration at FWHM, their spectral shape and bandwidth at FWHM, and their spectral phase and quality factor F. This factor is defined as the ratio of the nonlinear fluorescence signals produced by the calculated pulse and a reference pulse. The reference pulse has the same spectrum as the calculated one but with a spectral phase equal to the Fourier-transform-limited pulse.

3 Presentation and Analysis of the Numerical and Experimental Results

3.1 Numerical Evaluation of the Performances of Each Double-Clad Fiber

For these numerical simulations, we have considered 0.5 W from the oscillator. Each fiber is coupling 50% of the power and the grism line is transmitting 30%. Adjusting the grism line parameters d and θ allows to obtain the best quality factor and the shortest pulse duration at FWHM for each DCF. The results presented in Fig. 2 show the pulse duration and quality factor F for each DCF as a function of the distance d for a fixed angle θ, identified as the ideal orientation of grism line.

For each of the four DCFs, the calculated pulse duration is shorter than 40 fs. Considering the initial pulses from the oscillator, it highlights pulses four times shorter than the initial pulses. This parameter is fundamental, considering the importance of the shortest pulse duration for the safety and image quality of the tissue. These numerical results endorse the importance of the simultaneous compensation of SOD, TOD, and nonlinear effects. It validates the architecture composed of a first fiber, a grism line, and a DCF, as previously described.

The Crystal Fiber DCF gives the shortest pulse duration (23 fs) and the highest quality factor (64%). These results illustrate that the pulse duration is related to the size of the core. The smaller the core size, the higher are the nonlinear effects which distorting the spectrum. Identically, the quality factor decreases with the diameter of the fiber core.

For each of the four DCFs, the grism line position for the shortest pulse duration is shifted a few millimeters, compared

to the position with the highest quality factor. It is linked to the pulse duration which is measured at the FWHM, neglecting the shape of the pulse. Figure 3 presents the shape of the pulse from the Crystal Fiber DCF, calculated for the shortest pulse [22.7 fs, Fig. 3(a)] and for the highest quality factor [23.4 fs, Fig. 3(b)]. Indeed, the maximum of quality factor is obtained for the smallest pulse shape pedestal. Finally, the quality factor is maximized when the pulse energy is mainly contained into the central peak and a lowest level is lost in the pedestal. Consequently, the best multiphoton signal is obtained when the shortest pulse is, for example, at 10% of the maximum, considering the presence of the pedestal. In our case, the pulse duration at 10% of the maximum is 92.8 fs in Fig. 3(a) and 57.0 fs in Fig. 3(b).

3.2 Experimental Measurements Compared with Numerical Results and Literature

Pulses have been characterized experimentally at the output of each DCF and compared to numerical simulations that were presented in the previous section. Laser output pulses have a duration of 100 fs at FWHM at the central wavelength of 800 nm [Fig. 1(b)]. The optical characteristics of the delivered pulses at the endoscopic DCF output are measured experimentally. The four DCFs were successively placed in the position named "2 m DCF." Before this fiber, the average power is 80 mW.

The intensity autocorrelation trace, the spectrum, and average power coupled in each DCF core were measured. The negligible power coupled in the inner cladding has been verified. Figure 4 presents the autocorrelation traces [Fig. 4(a)] and the corresponding spectral shapes [Fig. 4(b)] obtained at the output of the four DCFs. Table 2 presents the values of optimal experimental pulse durations obtained by adjusting the DOF of the grism line while considering a secant hyperbolic square shape (sech^2) profile. Corresponding pulse energy and peak power were calculated. Table 2 summarizes the numerical results and experimental pulse durations obtained elsewhere in the literature using the same fibers. To complete our study, we have calculated the Fourier transform limit pulse of the
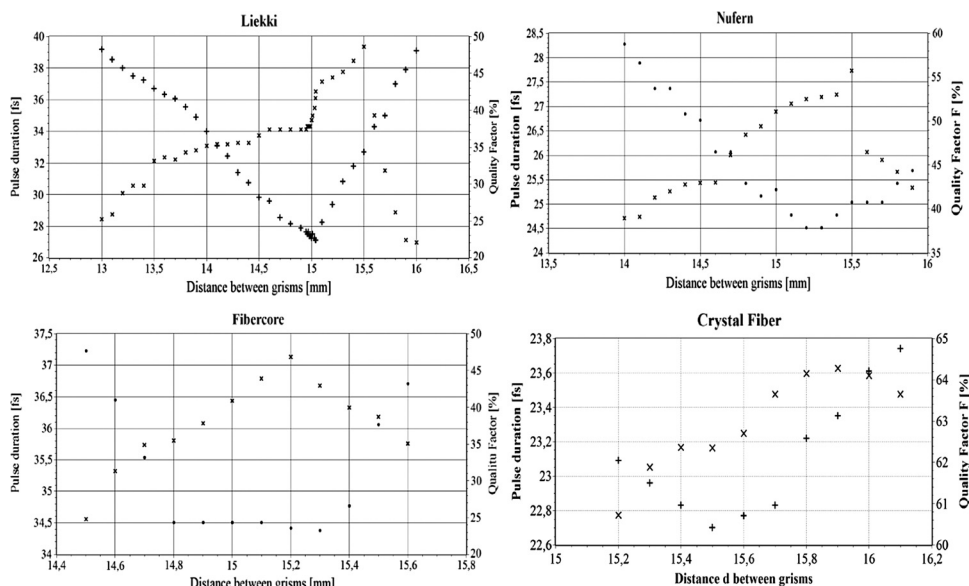

Fig. 2 Calculated pulse duration (FWHM) and quality factor at the output of each DCF. Crosses represent pulse duration. Points represent quality factor F.
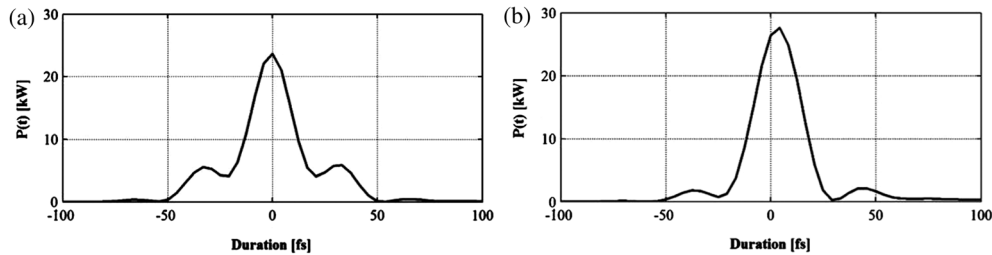
Fig. 3 Calculated pulse shapes at Crystal Fiber output. (a) Shortest pulse (FWHM): 22.7 fs and $F = 62.3\%$, (b) the highest quality factor $F = 64.3\%$ and 23.4 fs (FWHM).

experimental spectrum by considering a total compensation of dispersion, which gives the pulse shape and its shortest expected duration (i.e., with a flat spectral phase).

Overall, we obtained experimental pulse durations close to what was expected by simulation. Whatever the DCF used, sub-40-fs pulses were achieved. The comparison of these durations with the experimental results found in the literature confirms the importance of nonlinear effects and dispersion compensation up to the third order. Simultaneous compensation of SOD, TOD, and nonlinear effects was managed by the setup using a first fiber and a grism line, which resulted in the shortest pulse duration ever used in endomicroscopy (40 fs for the Liekki, 37 fs for the Fibercore, 31 fs for the Nufern, and 24 fs for the Crystal Fiber). Table 2 corroborates the numerical results about the best fiber for optimal pulse delivery except for Liekki DCF that suffered of nonlinear effects that were difficult to compensate experimentally. Considering pulse duration at Crystal Fiber DCF output (24 fs), oscillator repetition rate (80 MHz), and average power coupled into the core (50 mW), this DCF is giving 0.5 nJ of energy per pulse, with a 18.3-kW/cm^2 peak power. However, this fiber has a large core size, which can affect resolution. This drawback

Fig. 4 Pulse characterization at each DCF output. (a) Autocorrelation traces with the corresponding pulse duration FWHM in parenthesis considering a sech^2 profile, (b) corresponding spectral traces with the spectral width at FWHM between parentheses.

still needs to be investigated. From the standpoint of pulse duration, each of the four-tested DCFs can be adapted for nonlinear endomicroscopy with a preference for the DCF from Crystal Fiber.

3.3 Fluorescence Measurement at the Distal Position with the Double-Clad Fiber from Crystal Fiber

The objective of this part is to show the influence of the pulse duration and average power on the level of fluorescence emission. Among the four fibers experimentally tested, the fiber from Crystal Fiber has given the best excitation beam parameters at its output in terms of pulse duration and average power. We are able to reach around 50 mW at the output of the fiber, which is more than enough for exciting endogenous fluorophores of tissues with 25-fs duration. This fiber also theoretically presents the best characteristics of the inner cladding for multiphoton signal collection such as the largest inner cladding with high NA (see Table 1). Fluorescence collection via the Crystal Fiber was tested using a fluorescent solution. The ability of light pulses at the output of this fiber to generate a multiphotonic process is presented in Fig. 5.

Two tests were used to analyze the fluorescence signal. The first test allowed us to study the effect of the duration of the excitation pulses on the emitted fluorescence [Fig. 5(a)]. This measurement requires an initial step to measure the pulse duration at the DCF output as a function of the distance d between the grisms. This very repetitive experiment is introducing more or less uncompensated SOD and TOD. The second test was done by varying the output average power, while the shortest pulse duration of 24 fs is kept constant [Fig. 5(b)]. This has been managed by reducing the beam injected into the DCF.

As could be expected, the fluorescence level is higher for the shortest pulse duration [Fig. 5(a)] with the highest average power [Fig. 5(b)]. Indeed, the measurement of fluorescence without the sample at the DCF output shown at Fig. 5(b) is defining the level of dark current of the DCF from Crystal Fiber. This curve is not changing, increasing the power until the maximum of 50 mW. Consequently, no autofluorescence from the fiber is characterized. This result is explained considering the pure silica core composition of the DCF. The cladding index is reduced because of its mixed composition between air and silica in a microstructure. The beam propagation is consequently ensured by total internal reflection in the core. This experiment confirms the importance of using short pulse duration to enhance the fluorescent signal. This is important when we expect tissue imaging. The variation of the excitation power, for the shortest pulse duration, shows that it could be possible to reach 50 mW at the output of the DCF while keeping the same spectral shape and without expecting autofluorescence from the
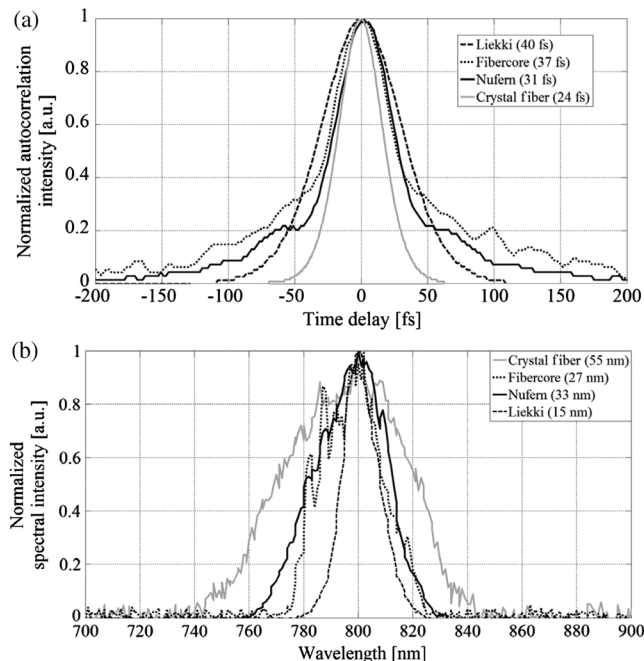
Table 2 Experimental results of pulse duration and average power at the endoscopic DCF output in the literature, compared to our experimental results and to numerical simulations. Calculation of experimental pulse energy and peak power. Pulse duration calculated from the Fourier-transform-limited pulse of the experimental spectrum with perfect dispersion compensation.

DCF	Minimum pulse duration				Average power		Pulse energy (nJ)	Peak power (kW/cm²)
	Literature	Numerical simulations (fs)	Exp. duration (fs)	Calculated from the exp. spectrum (Fourier limit) (fs)	Literature (mW)	Measured (mW)		
Liekki	150 fs[25]	27	40	36	20 mW[25]	9	0.11	2.42
Fibercore	1,5 ps[17] 130 fs[20] 200 fs[21]	34	37	33	30 mW[17] 15 mW[20] 50 mW[21]	5	0.06	1.43
Nufern	290 fs[22] 290 fs[23]	24,5	31	27	50 mW[22] 75 mW[23]	11	0.14	3.97
Crystal Fiber	100 fs[16] 260 fs[19] 1 ps[24] 290 fs[26]	22,7	24	19	40 mW[16] 15 mW[19] n.c.[24] 50 mW[26]	50	0.5	18.3

DCF. This power could be needed sometimes when a very weak intrinsic fluorescence from tissues is imaged.

4 Discussion and Conclusions

4.1 Few Technical Difficulties

The choice of an endomicroscopic DCF often falls on commercial fibers, as it is not easy to have access to homemade fibers that are suitable for endoscopic imaging. Hundreds of commercial DCFs are available with various parameters (core and cladding composition, size, NA, structure, etc.). Most of these fibers are rare-earth-doped and are mainly manufactured for amplified fiber lasers. These doped fibers can potentially produce a noise from the fiber itself, which can disturb the measurement of a very low level of fluorescence or SHG signals.

Laser injection in each of the four fibers was delicate. Each fiber has different characteristics: core diameter, core NA, and wavelength single-mode operation. This imposes an adjustment and always a replacement of the optics that were used for laser injection specifically for each case. Finding an ideal injection lens that can achieve high coupling efficiency was problematic. All fibers suffered a low level of injection except the DCF from Crystal Fiber. For each of the four DCFs, nine different optics were tested for injection. The ideal coupling should be effective knowing the best-adapted optical parameters (beam diameter, N.A. of the focalization objective, etc.) for injection in each of the fibers. The information has not been found experimentally

for the three DCFs (Nufern, Liekki, and Fibercore) giving less than 20% of injection.

A multimode delivery was also often observed, especially in the DCF from Nufern. This mode quality as single-mode operation is highly important to consider in order to impose an efficient nonlinear excitation. Maintaining single-mode delivery was possible by modifying the collimation at the first fiber output (Fig. 1). The beam size was adapted to this DCF input. Figure 6 represents the pictures of the delivery mode imaging at the DCF output from Nufern with a 20× microscope objective, replacing the Rhodamine cuvette [Fig. 1(a)] by a screen. Figures 6(a) and 6(b) show the beam shapes for a multimode delivery. Figure 6(c) presents the fundamental mode delivery resulting from the adaptation of coupling with the compression and precompensation unit. The single-mode operation was maintained whatever the fiber distortion: bending, twisting, or shaking.

4.2 Discussion on the Choice of the Ideal Double-Clad Fiber for the Endomicroscopic System

The DCF from Crystal Fiber, a microstructured fiber, turned out to be the best in terms of single-mode delivery of ultrashort pulses around 800 nm. Moreover, it has the smallest core NA and the highest inner cladding NA. These two parameters are substantial for delivering high-quality excitation pulses with a
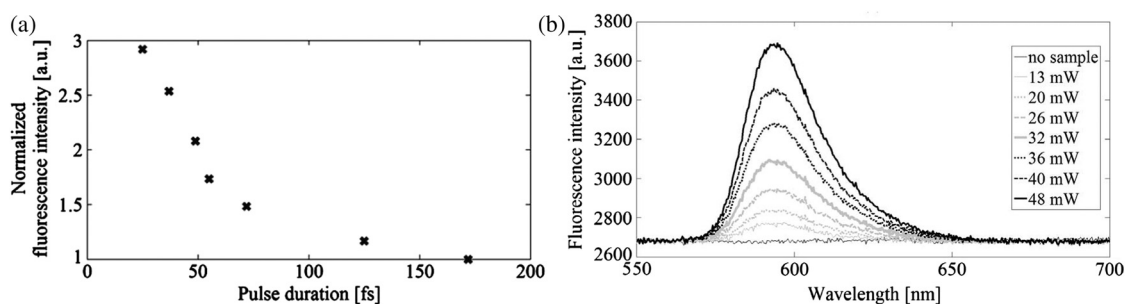

Fig. 5 Backward rhodamine TPF with the DCF from Crystal Fiber. (a) Fluorescence intensity as a function of the DCF output pulse duration, normalized to the TFP intensity at 172 fs, (b) rhodamine TPF as a function of the average power at DCF output. Dark current level of the DCF measured without sample at the DCF output.
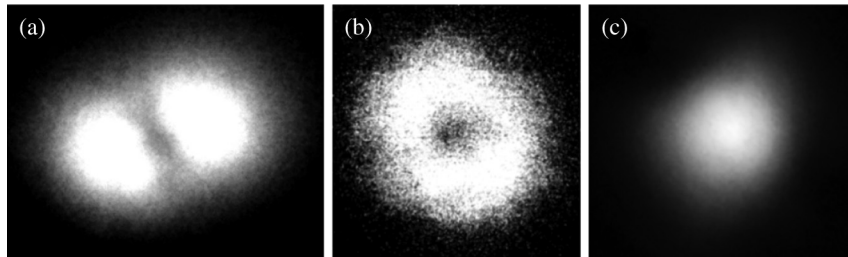
Fig. 6 Spatial profile of light exciting the fiber core of the DCF from Nufern. (a) LP11 mode, (b) a mixture between modes obtained bending, shaking, and twisting the DCF, (c) delivery of the fundamental mode of the light after adjusting the collimation at the first fiber output. No modification of the single-mode operation was observed after bending, twisting, and shaking the DCF.

low level of optical aberrations in the distal optics, and the highest level of nonlinear signal collection.

However, its core diameter is a real problem for the miniaturization of the distal optic and the resulting optical resolution, which is inevitably highly reduced, compared to a DCF with a smaller core. Moreover, the microstructured Crystal Fiber DCF is between 25 and 60 times more expensive than the others studied step-index DCFs. For the experimental tests of the prototype in laboratory, this point is not really problematic. But in a context of a clinical use, it can become a huge concern. Indeed, the requirement in several hospitals is to change the endoscopic part with a new, never-used one after each endoscopic exploration for hygiene purposes.

In another work soon to be published, a study of the miniaturized distal lens (gradient index lens) will be presented. It will highlight the dramatical decrease in resolution for the use of a large core DCF. A compromise between these parameters must be found to obtain the ideal endoscopic system characteristics.

5 Conclusion

In brief, we have presented a numerical and experimental comparison of four commercial DCFs that were used in the literature for nonlinear endomicroscopic systems. As the reason behind the choice of the DCF was not precisely justified, we have compared each of them in terms of output pulses quality and ability to produce multiphoton signals. A homemade numerical program was used and a test bench that allowed the compensation of linear and nonlinear effects of the system was built. To the best of our knowledge, we obtained the shortest pulse duration that has never been previously reported in the literature for each of the four DCFs. In the point of view of pulse duration, the ideal commercialized DCF is the one from Crystal Fiber. However, the choice of the ideal DCF depends on the level of miniaturization and the resolution required. A compromise must be made among the miniaturization of the distal optics, the desired optical resolution, and the collection efficiency.

References

1. M. Salaün et al., "In vivo imaging of pulmonary alveolar proteinosis using confocal endomicroscopy," *Eur. Respir. J.* **36**(2), 451–453 (2010).
2. W. Denk, J. H. Strickler, and W. W. Webb, "Two-photon laser scanning fluorescence microscopy," *Science* **248**(4951), 73–76 (1990).
3. B. A. Flusberg et al., "Fiber-optic fluorescence imaging," *Nat. Methods* **2**(12), 941–950 (2005).
4. L. Fu and M. Gu, "Fibre-optic nonlinear optical microscopy and endoscopy," *J. Microsc.* **226**(3), 195–206 (2007).
5. P. Xi et al., "Two-photon imaging using adaptive phase compensated ultrashort laser pulses," *J. Biomed. Opt.* **14**(1), 014002 (2009).
6. I. Saytashev et al., "Pulse duration and energy dependence of photodamage and lethality induced by femtosecond near infrared laser pulses in Drosophila melanogaster," *J. Photochem. Photobiol. B.* **115**, 42–50, (2012).
7. P. Xi et al., "Greater signal, increased depth, and less photobleaching in two-photon microscopy with 10 fs pulses," *Opt. Commun.* **281**, 1841–1849 (2008).
8. G. McConnell, "Improving the penetration depth in multiphoton excitation laser scanning microscopy," *J. Biomed. Opt.* **11**(5), 054020 (2006).
9. M. Lelek et al., "Coherent femtosecond pulse shaping for the optimization of a non-linear micro-endoscope," *Opt. Express* **15**(16), 10154–10162 (2007).
10. S. Ramachandran et al., "High-energy (nanojoule) femtosecond pulse delivery with record dispersion higher-order mode fiber," *Opt. Lett.* **30**(23), 3225–3227 (2005).
11. T. Le et al., "Routes to fiber delivery of ultra-short laser pulses in the 25 fs regime," *Opt. Express* **17**(3), 1240–1247 (2009).
12. P. Tournois, "New diffraction grating pair with very linear dispersion for laser pulse compression," *Electron. Lett.* **29**(16), 1414–1415 (1993).
13. C. Lefort et al., "Pulse compression and fiber delivery of 45 fs Fourier transform limited pulses at 830 nm," *Opt. Lett.* **36**(2), 292–294 (2011).
14. M. Kalashyan et al., "Ultrashort pulse fiber delivery with optimized dispersion control by reflection grisms at 800 nm," *Opt. Express* **20**(23), 25624–25635 (2012).
15. S. W. Clark, F. Ö. Ilday, and F. W. Wise, "Fiber delivery of femtosecond pulses from a Ti: sapphire laser," *Opt. Lett.* **26**(17), 1320–1322 (2001).
16. L. Fu et al., "Three-dimensional nonlinear optical endoscopy," *J. Biomed. Opt. Lett.* **12**(4), 040501 (2007).
17. H. Bao et al., "Second harmonic generation imaging via nonlinear endomicroscopy," *Opt. Express* **18**(2), 1255–1260 (2010).
18. G. Ducourthial et al., "Label free multiphoton imaging of human pulmonary tissues through two-meter-long microstructured fiber and multicore image-guide," *Proc. SPIE* **8575**, 85750H (2013).
19. W. Jung et al., "Miniaturized probe based on a microelectromechanical system mirror for multiphoton microscopy," *Opt. Lett.* **33**(12), 1324–1326 (2008).
20. Y. Wu et al., "Scanning all-fiber-optic endomicroscopy system for 3D nonlinear optical imaging of biological tissues," *Opt. Express* **17**(10), 7907–7915 (2009).
21. Y. Wu et al., "Scanning fiber-optic nonlinear endomicroscopy with miniature aspherical compound lens and multimode fiber collector," *Opt. Lett.* **34**(7), 953–955 (2009).

22. D. R. Rivera et al., "Compact and flexible raster scanning multiphoton endoscope capable of imaging unstained tissue," in *PNAS*, Vol. 108, pp. 17598–17603 (2011).
23. C. M. Brown et al., "In vivo imaging of unstained tissues using a compact and flexible multiphoton microendoscope," *J. Biomed. Opt.* **17**(4), 040505 (2012).
24. F. Knorr et al., "Two-photon excited fluorescence lifetime measurements through a double-clad photonic crystal fiber for tissue microendoscopy," *J. Biophoton. Lett.* **5**(1), 14–19 (2012).
25. Y.-C. Chang et al., "Fiber-optic multiphoton flow cytometry in whole blood and in vivo," *J. Biomed. Opt.* **15**(4), 047004 (2010).
26. G. Liu et al., "Rotational multiphoton endoscopy with a 1 μm fiber laser system," *Opt. Lett.* **34**(15), 2249–2251 (2009).
27. E. R. Andresen et al., "Toward endoscopes with no distal optics: video-rate scanning microscopy through a fiber bundle," *Opt. Lett.* **38**(5), 609–611 (2013).
28. D. G. Ouzounov et al., "Dual modality endomicroscope with optical zoom capability," *Biomed. Opt. Express* **4**(9), 1494–1503 (2013).
29. S. Brustlein et al., "Double-clad hollow core photonic crystal fiber for coherent Raman endoscope," *Opt. Express* **19**(13), 12562–12568 (2011).

Claire Lefort has expertise in femtosecond pulse delivery through optical fibers. She masters pulse precompensation with several passive of active tools. She has experience with the miniaturization of nonlinear microscopes giving an experience in nonlinear endomicroscopy. She is currently working as a researcher for the French CNRS.

Hussein Hamzeh received his BSc in general physics and MSc in medical imaging from the Lebanese University Faculty of Sciences. In 2012 he joined IMNC Laboratory in Orsay, France, as a master's student and later as a research engineer, where he worked on the development of nonlinear microendoscopy. Currently, he is doing his PhD at Caesar Research Center; an institute of the Max-Planck Society in Germany. His research focuses on revealing protein ultrastructure using super-resolution microscopy.

Frederic Louradour is the head of Biof3 project, which is part of the Photonics Department of XLIM UMR CNRS 7252 laboratory. His competencies belong to the fields of optical engineering, optical instrumentation, nonlinear optics, femtosecond technologies and optical fiber technologies. Biof3 recently performed high resolution *in vivo in situ* label free multiphoton imaging through a 5-m-long innovative optical fiber equipped with a 2.2-mm-diameter imaging probe.

Frédéric Pain has been an associate professor at Université Paris Sud Orsay since 2002. After initial work in the field of instrumentation for *in vivo* detection of radiolabeled molecules, he moved in 2006 to the field of *in vivo* optical imaging for the study of neuroenergetics using multispectral intrinsic optical imaging, dynamic laser speckle contrast imaging and dynamic imaging of flavoproteins autofluorescence. He recently got involved in the instrumental development of an endomicroscope dedicated to brain studies in a clinical context.

Darine Abi Haidar is an associate professor at Paris Diderot University and the director of the nonlinear optical imaging platform for small animals at IMNC Laboratory. She has a PhD in physics from Jean Monnet University of Saint-Etienne, where she worked in nonlinear optical microscopy and tissue characterization. She gained extensive experience in nonlinear endomicroscopy during her postdoctoral research. Her current research involves endomicroscopy development with focus on pulse precompensation, TPF and SHG signal optimization.